# Spin-polarization study of CO molecules adsorbed on Fe(110) using metastable-atom deexcitation spectroscopy and first-principles calculations

X. Sun,[1,2] S. Förster,[3] Q. X. Li,[2] M. Kurahashi,[1] T. Suzuki,[1,4] J. W. Zhang,[1,2] Y. Yamauchi,[1,*] G. Baum,[3] and H. Steidl[3]
[1]*National Institute for Materials Science, 1-2-1 Sengen, Tsukuba 305-0047, Japan*
[2]*Hefei National Laboratory for Physical Sciences at Microscale and Department of Physics, University of Science and Technology of China, Hefei, Anhui 230026, China*
[3]*Fakultät für Physik, Universität Bielefeld, D-33615 Bielefeld, Germany*
[4]*PRESTO, Japan Science and Technology Agency, 4-1-8 Honcho, Kawaguchi 332-0012, Japan*
(Received 12 September 2006; revised manuscript received 26 November 2006; published 19 January 2007)

The spin-resolved electronic states of CO molecules adsorbed on Fe(110) surfaces are investigated using spin-polarized metastable-atom deexcitation spectroscopy (SPMDS) measurements and first-principles calculation. The existence of the adsorbate-induced $2\pi^*$ state, which is partially filled by electron backdonation, is detected directly by SPMDS and reproduced by the calculation of local density of states and subtracted densities. Positive spin asymmetries for $4\sigma$, $5\sigma/1\pi$, and $2\pi^*$ peaks observed in SPMDS spectra are well described by the calculated spin density and plane-averaged density of states, which indicate negative-spin polarization towards vacuum side even at the low CO coverage.

DOI: 10.1103/PhysRevB.75.035419 PACS number(s): 71.15.Mb, 73.20.At, 79.20.−m, 75.25.+z

## I. INTRODUCTION

The interaction between molecules and transition-metal surfaces has attracted much attention leading to numerous experimental and theoretical investigations. This is due to the fact that, adsorption and dissociation of molecules on transition-metal surfaces play an important role in many catalytic processes. Moreover, new electronic states have been proposed to be formed at the molecule (metal) interface near the Fermi level ($E_F$). One of the well-known examples is the backdonation of metal electrons to an adsorbed CO $2\pi^*$ orbital.[1] Several experimental techniques, including electron-energy loss spectroscopy,[2,3] x-ray photoelectron spectroscopy,[3,4] and ultraviolet photoelectron spectroscopy (UPS)[5] etc., have been used to investigate the electronic structure of adsorbate-covered metallic surfaces. Among these UPS has been proven to be an almost ideal technique for the determination and the assignment of the valence level of the adsorbate. However, the adsorbate-induced state (AIS) around the $E_F$ is difficult to detect (even with UPS) due to the obscuring by the strong emission from the substrate *d* band. Unlike UPS, metastable-atom deexcitation spectroscopy (MDS) can detect the AIS on the surface more sensitively than valence electronic states in deeper layers, since deexcitation involves electrons distributed outside of the surface. With the addition of spin polarization, this technique (SPMDS) provides an extremely sensitive tool to study the spin-resolved electronic structure of the adsorbate and magnetic surface. An evident and well-studied case is the adsorption of oxygen on Fe films. A change of sign in the asymmetry of spin polarization right below $E_F$ has been found with oxygen exposure above 3 L.[6–8] SPMDS has also been used to investigate complicated systems such as water and sodium coadsorption on the Fe film,[9] and organic molecules such as pentacene on the magnetic Fe substrate.[10]

In this paper, we report the spin-polarized density-functional theory (DFT) calculations together with the SPMDS measurements for CO adsorption on the Fe/W(110) surface. The SPMDS results can be compared with the spin density and plane-averaged density of states (PDOS) in the vacuum region, since SPMDS probes predominantly the electronic states extending towards the vacuum side of the topmost surface.[11] The selection of the system of CO/Fe(110) is due to the following reasons. One is the significant importance of this system involved both in fundamental investigation and industrial application. Another is that the relative simple electronic structure of CO is helpful to discuss the AIS and the electron donation and backdonation. Moreover, previous studies of the CO/Fe(110) system focused mainly on the adsorption geometry and dissociation process.[12–14] The spin-resolved electronic structure of CO adsorbed on the Fe(110) surface has not been fully illuminated yet either by experimental investigation or through theoretical research. Our study reveals the magnetic interactions between CO and the substrate.

Our measurements show that considerable spin polarization has been observed not only at the MDS peaks coming from CO $4\sigma$ and $5\sigma/1\pi$ states, but also the $2\pi^*$ state with an especially higher value. These experimental SPMDS results can be reasonably explained by the calculated spin density and PDOS in the vacuum region. The electron backdonation from the Fe substrate to the adsorbed CO $2\pi^*$ orbital will also be clearly highlighted by the subtracted density map.

## II. EXPERIMENTAL TECHNIQUES

The experimental setup is described in Refs. 15 and 16 in detail. Here we will give only a short overview of the main points. The He($2^3S$) beam is produced by a discharge source and polarized by means of a sextupole magnet, reaching spin polarization of about 90%. A spin flipper is used to reverse the direction of polarization. Its efficiency is determined to be very close to 100%, so it is ensured that one obtains equal beam polarization for the reversed and the nonreversed case. The experiment is performed in an UHV chamber with a base pressure in the upper $10^{-11}$ mbar range.

 

A W(110) crystal serves as the target substrate and is cleaned by heating in oxygen and flashing up to 2600 K. The iron films are applied by means of an electron-beam evaporator in the low $10^{-10}$ mbar pressure range. An integrated flux monitor facilitates a reproducible growth rate, typically a third of a monolayer per minute. The quantity of the evaporated iron can hereby be controlled to better than 5%. The thickness of the films is typically about 20 Å. Subsequent annealing of these films to about 400 K leads to patterns corresponding to well-defined bcc iron (110) surfaces, as is seen by means of low-energy electron diffraction (LEED). In these films the surface anisotropy causes the easy magnetization axis to lie in-plane along the $[1\bar{1}0]$ direction of the substrate. The films are uniformly magnetized in this direction, collinear to the atomic-beam polarization, by a current pulse through a coil situated close to the sample.

After preparation of the surface carbon monoxide exposures are done by means of inserting gas through an adjustable leak valve. Exposure is denoted in units of Langmuir ($1\ L \triangleq 10^{-6}$ Torr S), where 1 L is attained by rising CO partial pressure to $1.33\times10^{-7}$ mbar for 10 s.

The atomic-beam direction has an angle of incidence $\Theta = 30°$ with respect to the surface normal of the target. All spectra are taken in normal emission with an angular resolution of ±5°. The energy of emitted electrons is analyzed by a 150° spherical spectrometer with a radius of 100 mm. The energy resolution is set to about 160 meV. Transmitted electrons are detected by a channel-electron multiplier.

We take measurements with parallel ($I_p$) and antiparallel ($I_a$) spin orientations of the atomic-beam electrons related to the majority electrons of the ferromagnetic surface. We define the asymmetry $A$ of ejected electrons by $A=(1/P_A)[(I_p-I_a)/(I_p+I_a)]$, assuming that full single-domain magnetization of the target is preserved. $P_A$ is the polarization of the atomic beam. Because of the *opposite* polarization of the He($2^3S$)-1*s* hole, which is effective in the interaction, a *positive* asymmetry $A$ indicates a dominance of minority electrons, namely, *negative*-spin polarization.

## III. EXPERIMENTAL RESULTS AND ANALYSIS

Figure 1 shows the experimental SPMDS spectra (a) and spin asymmetry (b) for CO adsorption on Fe(110) surfaces in dependence on CO exposure. In general, two different deexcitation channels must be considered for the metastable $He^*$ atom. If the work function of the surface is larger than the ionization potential of $He^*$, the deexcitation mechanism is described by a resonant ionization with a subsequent Auger neutralization (RI+AN). Alternatively, RI is suppressed and a direct Auger deexcitation (AD) may occur as the dominant mechanism, if the work function is smaller or if the wavefunction overlap of the He($2^3S$)-2*s* electron with empty states at surface is insufficient due to an adsorbate layer. In the AD process the 1*s* hole of the He($2^3S$) atom is filled by an electron from the surface and the 2*s* electron is ejected with a kinetic energy of $E_{kin}=E^*-E_B-\phi$ ($E^*$ effective-excitation energy of $He^*$, $E_B$ binding energy of electron, $\phi$ work function). Since the spatial distribution of wave functions of surface-electronic states influences the ejection probability, it is not straightforward to estimate the exact value. Assuming equal-ejection probability for electronic states at the major deexciting position,[17] however, the SPMDS spectra in the AD process mostly reflect the density of occupied surface electronic states at around the interaction surface for $He^*$. In contrast, the AN process involves two surface electrons (at the energy level of $E_{B1}$ and $E_{B2}$), one which fills the $He^*$ 1*s* hole and one which is ejected with the excess kinetic energy of $E_{kin}=E^*_{1s}-E_{B1}-E_{B2}-2\phi$ ($E^*_{1s}$ effective 1*s* energy of $He^*$). Consequently, in this case the spectra reflect a convolution of the "effective" (i.e., transition probability weighted) corresponding surface density of states (DOS).[8] Due to the different energy relations for the AD and RI+AN processes the corresponding features in the spectra, especially the high kinetic-energy onset at the Fermi level, are located at different kinetic energies.

For the clean Fe surface the main deexcitation process is RI+AN.[18] The Fermi edge for the AN process is determined to be around 13 eV. Deconvolution of the spectra by means of an algorithm described in Ref. 7 yields the transition-probability-weighted DOS, which are effective in the AN process. This is shown in Fig. 1(c) (top panel). The result resembles features that are also seen in spin-polarized UPS,[24] namely, a peak with positive asymmetry in the energy region of −2.0 eV to $E_F$, followed by a shoulder with negative asymmetry down to −3.0 eV.

Up from exposures of 1 L, peaks corresponding to electron ejection from orbitals of CO appear and dominate the spectra for exposures from 3 L onwards. Concurrently, another Fermi edge at 14.5 eV is visible indicating the presence of the AD process [see the right-hand side of Fig. 1(a)]. Fe-3*d* emissions through RI+AN decrease with increasing CO exposure as is indicated by the drop of intensity around 12 eV. Their vanishing at exposures of 3 L and higher denotes that the CO layer completely shields the metal surface. The change of the work function of the surface due to the adsorbed CO is reflected by a variation of the AN Fermi edge from 13 eV (0 L) to 12.5 eV (1 L) and to 12 eV (≥1.5 L) and a corresponding change of the low kinetic-energy cutoff around 0 eV. This is consistent with the previously reported increments of the work function by 0.9–1.6 eV.[19–23]

Up from an exposure of about 3 L the spectrum of CO is well defined and shows peaks in terms of CO orbitals, prominent at about 7 eV (originating from $5\sigma/1\pi$ CO orbital), 4 eV ($4\sigma$) and 1.5 eV (no match to CO orbitals). This was also found by Ref. 25 in a study of the CO/Ni(111) system. For the 1.5 eV peak, the maximum of the asymmetry at 0.9 eV does not coincide with the intensity maximum. This indicates that the structure is not fully resolved due to the low kinetic-energy cutoff. Contrary to UPS spectra, a peak appears at an electron kinetic energy of about 13 eV in the region where the 3*d* electrons of the clean Fe surface should emit, but the CO shields the metal surface, indicated by the finding that the emission around 13 eV increases as the CO coverage increases. With CO/Fe/W(110), thoroughly studied by UPS,[24] this 13 eV feature is missing in the UPS spectrum. In Ref. 25 this feature is assigned to AD from the antibonding $2\pi^*$ orbital of CO, which is partly filled by the "backbonding donation" of electrons from the substrate

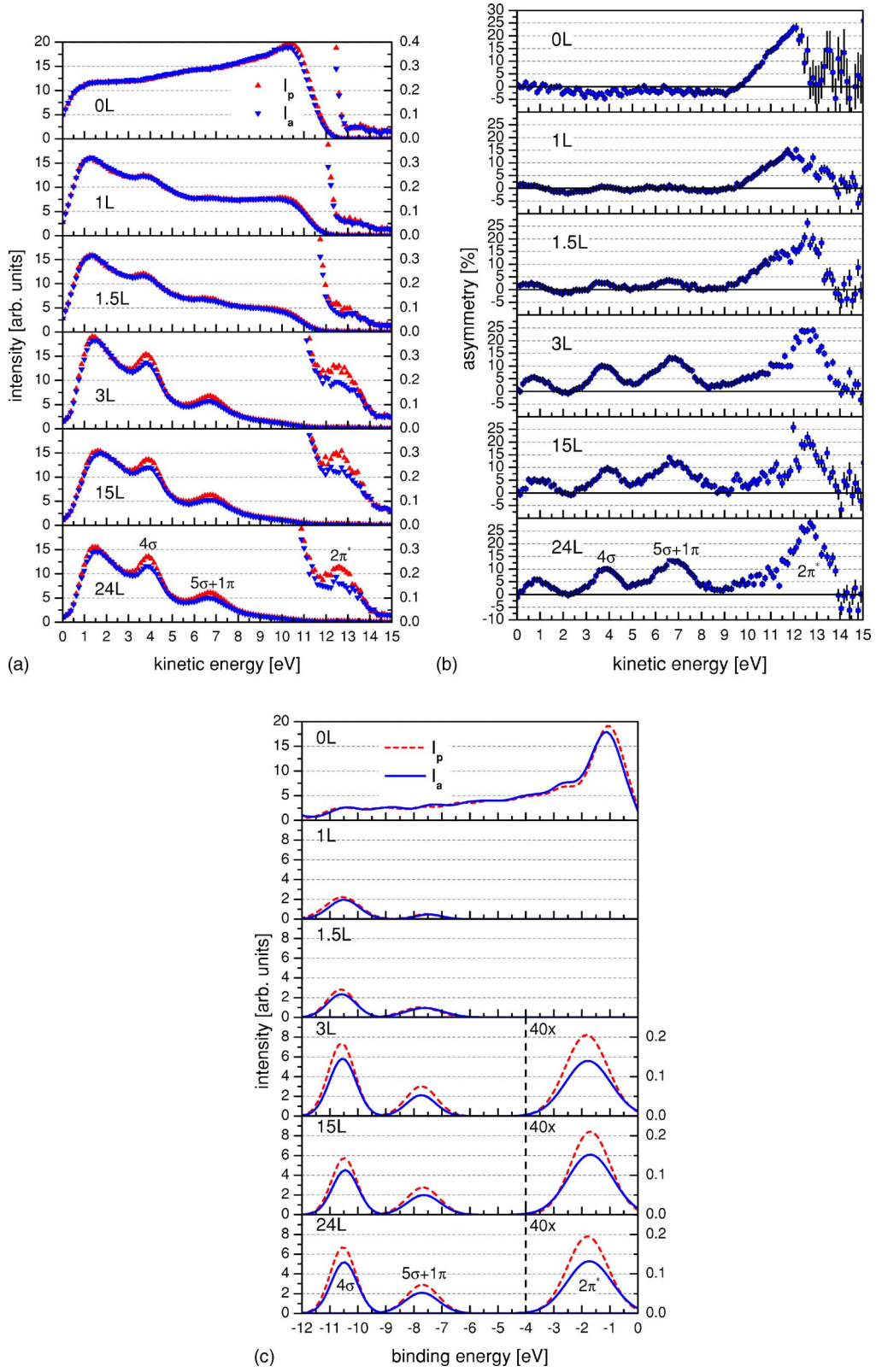


FIG. 1. (Color online) (a) The experimental SPMDS spectra for parallel ($I_p$) (red up triangle) and antiparallel ($I_a$) (blue down triangle) spin orientation, (b) spin asymmetry, (c) unfolded SPMDS spectra (top panel) and background-adjusted AD spectra (lower five panels) of CO adsorbed on Fe/W(110) at CO exposure of 0, 1.0, 1.5, 3.0, 15, and 24 L.

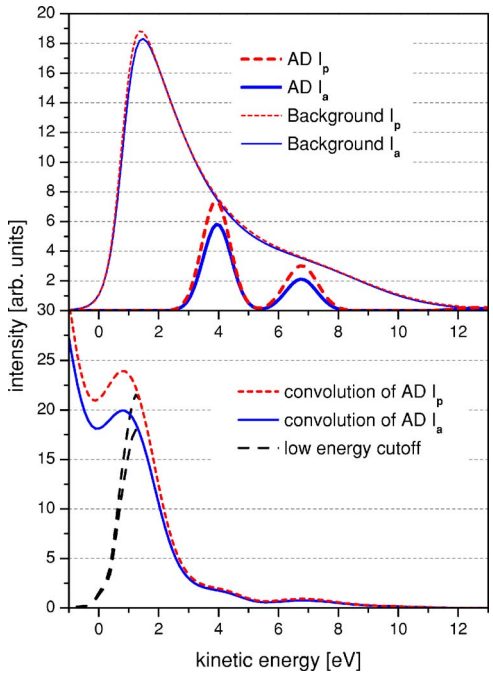


FIG. 2. (Color online) Background fit and background-adjusted AD part of spectra (upper panel) and convoluted AD spectra (lower panel) for 3 L.

metal. Our SPMDS investigation has revealed for the first time an asymmetry of these electrons occupying the $2\pi^*$ state, giving evidence of a dominance of minority electrons in this state, as well as the $5\sigma/1\pi$- and $4\sigma$-state in the CO/Fe/W(110) system [see Fig. 1(b)].

Similar to Ref. 25, the peaks are superimposed by a strong background, rising towards lower kinetic energies. According to angle-resolved measurement,[29] most AD electrons from the CO-derived states are emitted to the backward direction of the incident $He^*$, so that the background could not primarily be attributed to secondary electrons. The sharp onset (Fermi edge) around 12 eV indicates the presence of the RI+AN process even at the fully CO-covered surface. The $2\pi^*$ state of CO may manifest itself in a broad structure centered near the Fermi level. So RI takes place by tunneling of the $He^*$ 2*s* electron into the empty part of the $2\pi^*$ orbital. The contribution to the spectra reflects a convolution of the CO DOS. After implementing background fitting and subtraction [results shown in the lower five panels of Fig. 1(c)], we convolute the adjusted spectra (shown in Fig. 2) for 3 L exemplarily. Taking into account the low-energy cutoff, the RI+AN process gives a strong, noncoincident contribution to intensity and asymmetry in the range of 0–4 eV and smaller contributions from 6–9 eV. So the peak at 1.5 eV can be attributed to RI+AN. The lower value of asymmetry compared to the $4\sigma$ and $5\sigma/1\pi$ peaks indicates that the above-described mechanism is not the only one that contributes to the low-energy ejection. Another suggested mechanism[25] is the AN of the $CO^+$ ion left after $He^*$ impact. The electrons emitted by AN of the $CO^+$ ions with $5\sigma/1\pi$ holes will enhance the electron quantity in the low-energy region for both parallel and antiparallel spin orientation, thus the asymmetry of the 1.5 eV peak is reduced. Additionally, the lower value of asymmetry can also be connected with the two-hole correlation in AN. The two electrons involved in AN are known to prefer an antiparallel spin configuration at paramagnetic surfaces.[26] This antiparallel correlation will reduce the positive SPMDS asymmetry.

Contrary to measurements on other strongly chemisorbed CO systems CO/Pd(110) (Ref. 27), CO/Ni(111) (Ref. 28), the $5\sigma/1\pi$:$4\sigma$ intensity ratio is about 1:2.3 instead of 1.5:1 for CO/Pd(110) and 1.9:1 for CO/Ni(111), respectively. This must be attributed to the experimental geometry, i.e., the 30° angle of $He^*$ incidence as the emission from the $5\sigma/1\pi$ levels exhibits a pronounced angular structure.[29] Especially for angles of incidence above 20° $5\sigma/1\pi$ emission shows a minimum in normal direction whereas $4\sigma$ emission has a maximum in this direction regardless of the angle of $He^*$ incidence. The FWHM is about 0.46 eV for the $4\sigma$ peak, about 0.58 eV for $5\sigma/1\pi$, and about 0.75 eV for $2\pi^*$, respectively. Some broadening is to be considered since the effective excitation energy of $He^*$ in the AD process depends on the surface distance. This applies especially to low coverages of CO at which a higher FWHM is observed consequently.

## IV. THEORETICAL METHODS

First-principles study is conducted to investigate the spin-resolved electronic states of the CO molecule adsorbed on the Fe(110) surface and discuss the preceding experimental findings. All calculations are performed within the framework of DFT using a plane-wave basis set, as implemented in the Vienna *ab initio* simulation package (VASP).[30,31] Exchange-correlation interactions are described by the Perdew-Burke-Ernzerhof-generalized gradient approximation (GGA).[32] The projector-augmented wave method in its implementation of Kresse and Joubert is used to represent the electron-ion interaction.[33,34] The spin interpolation of Vosko *et al.* is adopted for spin-polarized calculations. The Brillouin-zone integration is calculated with an $8\times6\times1$ *k*-points grid, which is automatically generated using the Mokhorst-Pack method.[35] The plane-wave energy cutoff is set to 400 eV for all the calculations.

The Fe(110) surface is known to be the closed-packed surface with very slight relaxation.[36,37] In our calculation, a supercell with 36 Fe atoms is used to model the surface in which there are nine atomic layers and a vacuum region of 16 Å. CO molecules adsorb symmetrically on both terminated surfaces, as shown in Fig. 3. During the structural optimizations, we fix the central five atomic layers in the bulk configuration and allow all other atoms in the supercell to relax until all forces vanish within 0.01 eV/Å.

## V. THEORETICAL RESULTS AND DISCUSSION

### A. Adsorption geometry

We start with the geometric structure of bulk Fe and an isolated CO molecule. The GGA calculation yields a lattice constant and magnetic moment for bulk bcc Fe with 2.833 Å and $2.2\mu_B$/atom, which agree well with the experimental value of 2.866 Å and $2.22\mu_B$ (Ref. 36), respectively. The

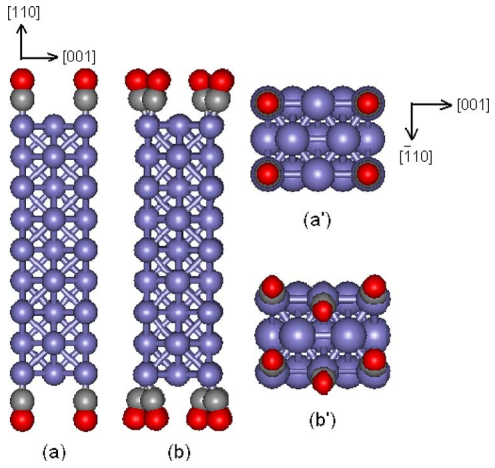


FIG. 3. (Color online) Computational models of CO/Fe(110). (a) and (a′) side and top view with the CO coverage of 0.25 ML. (b) and (b′) side and top view for the 0.5 ML case. The gray, red, and blue spheres stand for C, O, and Fe atoms, respectively.

optimized equilibrium CO bond length is 1.143 Å, which almost reproduces the experimental value (1.128 Å).[38] To investigate the adsorption behavior of CO molecules on Fe(110) surface, here, we concentrate on the submonolayer case including two different coverages with 0.25 and 0.5 ML CO molecules absorbing on the Fe(110)-$c(2\times4)$ surface. To find the most stable adsorption configuration, CO adsorption at atop, long-bridge, and short-bridge sites are considered in our calculations. The adsorption energy and optimized geometrical parameters at each site are shown in Table I. For the 0.25 ML case, CO molecules are predicted to prefer the atop site of the Fe(110) surface and stand there uprightly, which agrees with experimental observations and previous theoretical calculations.[12,14,39] Ours calculated the most stable configuration for the 0.5 ML coverage, CO molecules located at the long-bridge site, which is similar to Stibor's result.[14] For this case, their theoretical CO stretch frequencies ($1810\ cm^{-1}$) are much less than the experiment value ($1985\ cm^{-1}$). Low-energy electron diffraction and high-resolution electron-energy-loss spectroscopy data suggest that CO molecules still adsorb on the atop site but with a distorted configuration.[39] One reason for this discrepancy may originate from that the present implementations of DFT overestimate the adsorption energy for the high metal-coordinated site with respect to the low-coordinated position, which has been demonstrated clearly in the case of CO adsorption on Pt(111).[40] Another possible reason may be due to the temperature effect. The calculations are completed on the assumption that the temperature is 0 K, while experiments are performed at room temperature. Starting from a distorted initial configuration shown in Fig. 3(b) and 3(b'), our calculation confirms that the adsorption energy is indeed lowered about 38.6 meV with tilted CO molecules than the upright one. The tilting angle is about 11.3° with respect to the surface normal direction, which is close to the value (13°) predicted by Jiang and Carter's calculation.[37] It has been demonstrated by both experimental and theoretical studies that tilted adsorption geometry is a common phenomenon for CO adsorption on a metal surface, such as on Fe(100), Ni(110), and Pd(110) surfaces.[3,41,42] This tilting is probably caused by steric repulsion among adsorbed CO molecules, which becomes larger with the coverage increase and the CO-CO distance decrease.

### B. Electronic structure

Figure 4 shows the local DOS inside atomic spheres of the O, C, carbon-bonding Fe atom, and the corresponding surface Fe atom before CO adsorption as well as the total DOS of a free CO molecule, where the $E_F$ is shifted to zero. It is clear that for an isolated CO molecule three peaks below the $E_F$ correspond to $4\sigma$, $1\pi$, and $5\sigma$, respectively, while the antibonding $2\pi^*$ state locates above the $E_F$, which agrees well with a previous report.[43] When CO molecules adsorb on the Fe(110) surface, the position of molecular orbital shifts and local DOS is broadened due to the molecule-substrate and molecule-molecule interactions. The shoulder at −6.2 eV comes from the $5\sigma$ band, which shifts downwards significantly and energetically overlaps with the $1\pi$ band. The $2\pi^*$ orbital, which is empty in a free CO molecule, is now partially occupied after adsorption. The spin-resolved local DOS of O and C atoms is different between spin up and down, especially for the $2\pi^*$ state. The predicted spin polarization of the CO molecule originates from interaction with the strongly magnetic Fe surface. Comparing with the corresponding clean surface Fe atom, three peaks locating at −8.9, −6.3, and −5.9 eV in the local DOS of the Fe atom bonding to the C atom are induced by the $4\sigma$, $5\sigma$, and $1\pi$ states of the CO molecule. The peak at −5.9 eV is slightly lower in inten-

TABLE I. The calculated adsorption energy ($E_{ad}$) and geometric parameters for CO adsorption on Fe(110) with coverage of 0.25 and 0.50 ML.

| Site | Coverage | $E_{ad}$ (eV) | $d_{C\text{-}O}$ (Å) | $d_{C\text{-}Fe}$ (Å) | $d_{Fe\text{-}O}$ (Å) | h (Å) |
|---|---|---|---|---|---|---|
| Atop | 0.25 | −2.002 | 1.1734 | 1.7728 | 2.9462 | 1.7728 |
| Long bridge | 0.25 | −1.921 | 1.2019 | 2.3683 | 3.1762 | 1.2626 |
| Short bridge | 0.25 | −1.721 | 1.1871 | 1.9508 | 2.9699 | 1.5188 |
| Atop | 0.50 | −1.739 | 1.1734 | 1.7728 | 2.9462 | 1.7728 |
| Atop (distorted) | 0.50 | −1.778 | 1.1719 | 1.7858 | 2.9573 | 1.7376 |
| Long bridge | 0.50 | −1.816 | 1.1922 | 2.3663 | 3.1658 | 1.2589 |
| Short bridge | 0.50 | −1.498 | 1.1826 | 1.9415 | 2.9491 | 1.4921 |

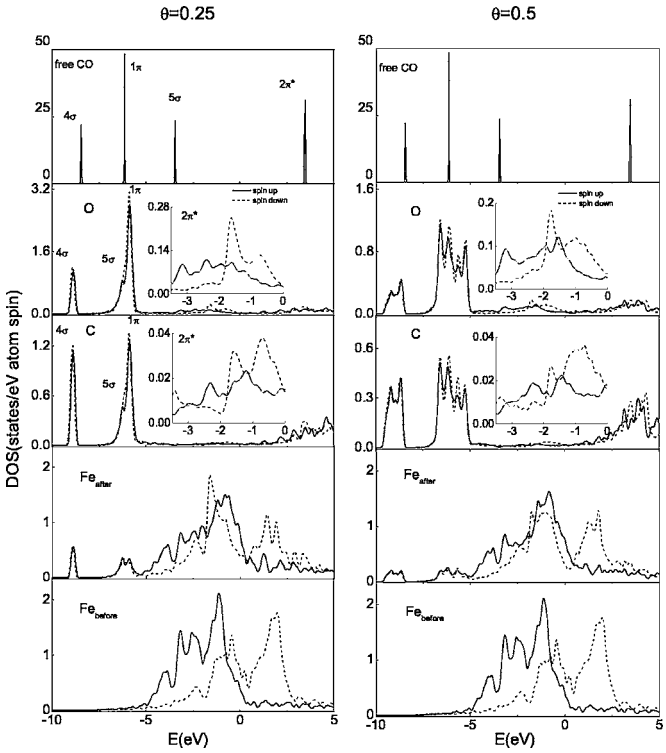


FIG. 4. The total DOS of an isolated CO molecule (with a broadening factor of 0.01), and local DOS inside the atomic sphere of the O, C, and Fe atom before and after CO adsorption. The right and left panel stand for the CO coverage of 0.25 and 0.5 ML, respectively. The dashed and solid curves are for spin-up and spin-down electrons, respectively.

sity than that of −6.3 eV one. The reason is that the $1\pi$ band of CO deriving from $p_x$ and $p_y$ orbitals of O and C atoms has a relatively weak interaction with the substrate, while the $5\sigma$ band bonds to the surface Fe atom strongly with its $p_z$ orbital. The local DOS(↓) of the carbon-bonding Fe atom below the $E_F$ increases obviously, while that of the neighboring Fe atom of the surface layer decreases slightly after the adsorption of the CO molecule. These result in the significant reduction of the magnetic moment of the carbon-bonding Fe atom from 2.58 to $1.19\mu_B$ and the small increment of that neighboring Fe atom to $2.73\mu_B$. The decrease in magnetic moment has also been theoretically predicted in CO chemisorbed on $\gamma$-Fe/Cu(100) and Ni(110).[44,45] With increasing the CO coverage from 0.25 to 0.5 ML, from the left panel of Fig. 4, the split and broadening of the CO-derived peaks are observed in the calculated local DOS. The variations are expected because of the tilting of the adsorption orientation and the enhanced CO-CO interaction.

The molecule-substrate interaction causes significant electron donation and backdonation processes, which involves the emptying of the $5\sigma$ orbital and filling of the $2\pi^*$ state, respectively.[46] To observe them, we calculate the subtracted densities according to the following formula:

$$\Delta n = n(\mathrm{CO/Fe}_{substrate}) - n(\mathrm{Fe}_{substrate}), \qquad (1)$$

here, $n(\mathrm{CO/Fe}_{substrate})$ and $n(\mathrm{Fe}_{substrate})$ are the charge density of the CO/Fe(110) configuration and the Fe substrate

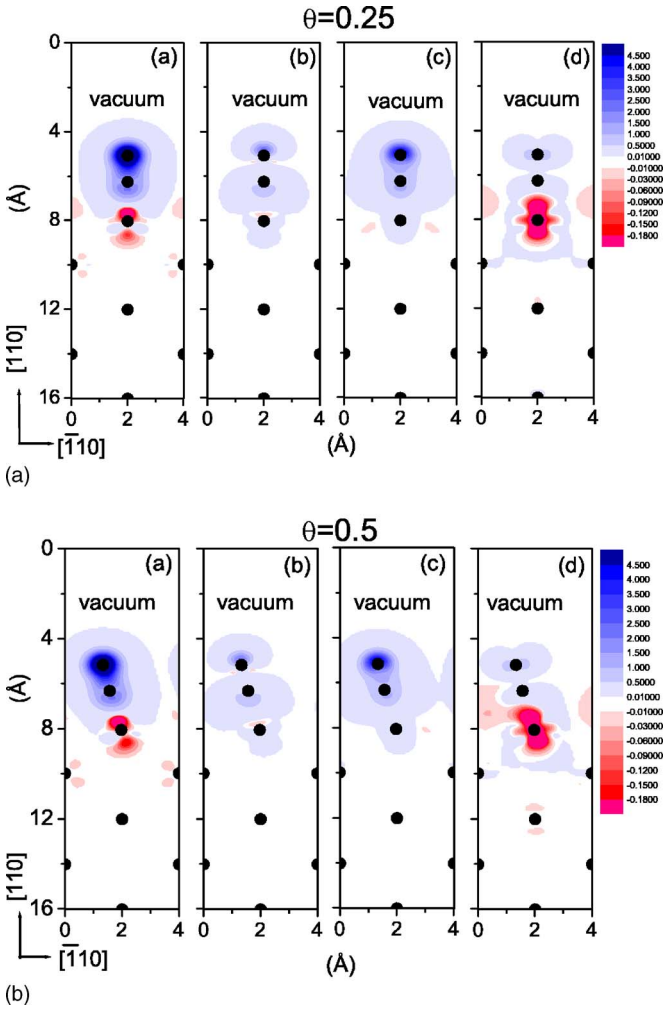


FIG. 5. (Color online) (a) The charge-density difference ($\Delta n$) of the CO/Fe(110) adsorption system with the whole energy region below $E_F$, [(b)–(d)] for $4\sigma$, $5\sigma/1\pi$, and $2\pi^*$ energy windows. The top and bottom panels stand for the CO coverage of 0.25 and 0.5 ML, respectively.

with the same geometric structure of the adsorption system, respectively. The calculated results along the (001) plane (which is vertical to the Fe(110) surface) are shown in Fig. 5. The blue and red color indicate the gain and loss of electron, respectively. The black-filled spots stand for C, O, and Fe atomic sites. Figure 5(a) shows the subtracted density in the whole energy region below $E_F$, (b)–(d) presents the $\Delta n$ lying in the $4\sigma$, $5\sigma/1\pi$, and $2\pi^*$ energy windows, respectively, which corresponds well to the spatial distribution of free CO molecular orbitals. The charge transfer between the Fe substrate and the CO molecule can be observed clearly from the density variation around the carbon-bonding Fe atom. For example, at $4\sigma$ and $5\sigma/1\pi$ states (shown in Figs. 5(b) and 5(c), respectively), the blue color suggests the net charge gain, indicating the electron donation from the CO molecule to Fe. In Fig. 5(d), at the $2\pi^*$ state, the red color obviously gives an evidence of the electron backdonation from the Fe substrate to the CO molecule. Similar results are obtained when the CO coverage increases to 0.5 ML. The main difference is the reduced electron backdonation. As a result, the

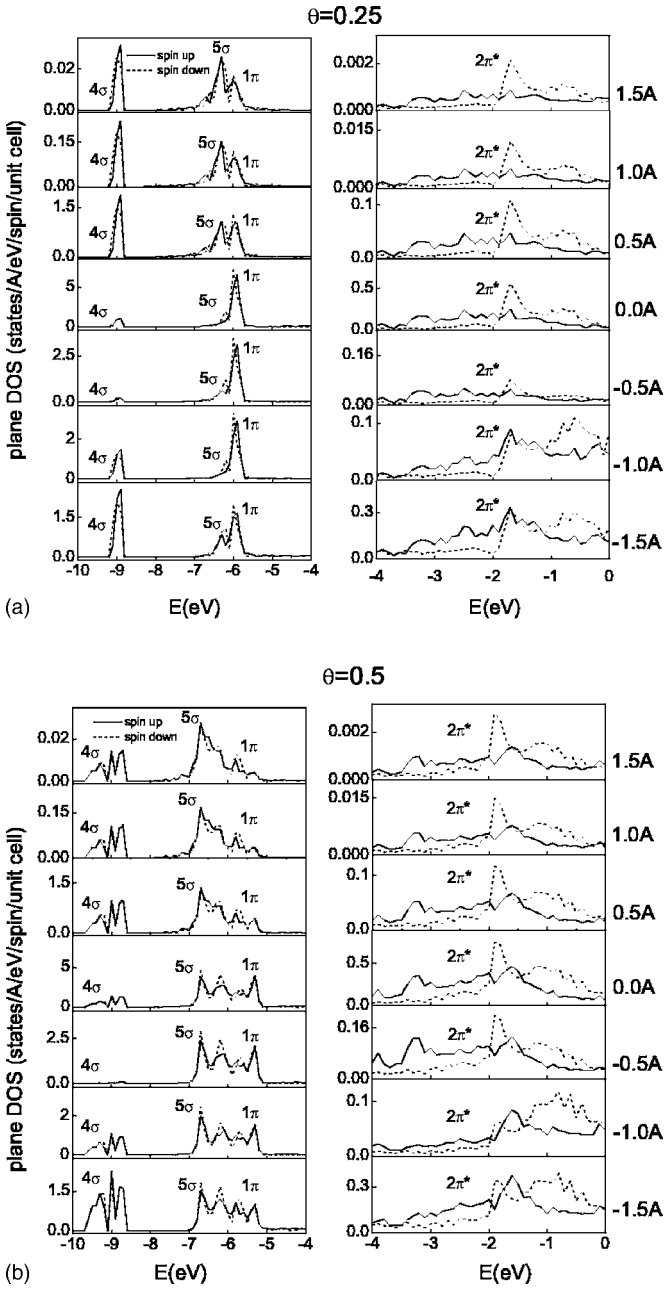


FIG. 6. The PDOS of CO/Fe(110) with various heights. The top and bottom panels stand for the CO coverage of 0.25 and 0.5 ML, respectively. The distances shown are those from the center of the oxygen atom.

Fe-C bond is a little weakened and the CO bond strengthened, as indicated with their bond length in Table I.

### C. Spin polarization

Since the SPMDS spectra reflect the electronic property extending toward the vacuum, the PDOS paralleling to the substrate surface with different heights are helpful to discuss the experimental SPMDS results.[47] Figure 6 shows the calculated PDOS at various distances from the surface with CO coverage of 0.25 and 0.5 ML. The height of PDOS is relative to the center position of the O atom. The positive (negative) value means that the plane locates at the vacuum (substrate) side of O atoms. It is clear that the $4\sigma$, $5\sigma/1\pi$, and $2\pi^*$ states can be assigned easily in the PDOS and the peak intensity decays approximately in an exponential way with increasing its height. At the plane of the O atom position, the relative intensity of the $4\sigma$ state is lower than that of $5\sigma/1\pi$, while this trend is reversed at the vacuum side due to the $p_z$ orbital of the O atom belonging to the $4\sigma$ state. The PDOS ($\downarrow$) is shifted to low energy slightly. The integration of PDOS indicates the dominance of the spin-down state thus a negative spin polarization at this state. For $5\sigma/1\pi$ states, the relative intensity of $1\pi$ is larger than $5\sigma$ at and below the center of the O atom, while it becomes smaller at the vacuum side. This result suggests that the $5\sigma$ state extends toward the vacuum region, while $1\pi$ locates mainly below the O atom and contributes to the C-O bonding. Compared with the PDOS($\uparrow$), the peak of PDOS($\downarrow$) of the $5\sigma$ state shifts to high energy and the $1\pi$ state moves towards low energy. The peak shift of PDOS may be caused by the difference in the spatial distribution of spin-up and spin-down electrons. The spin-down electrons belonging to the $4\sigma$ state have a larger density than that of spin up near the center of the O atom [Fig. 7(b)]. As a general rule, the binding energy should be higher for electrons that are located closer to the nucleus, resulting in the downward shift of the PDOS($\downarrow$) of the $4\sigma$ state. The shifts of PDOS of the $5\sigma$ and $1\pi$ states are also due to the dominance of the electron densities of $5\sigma(\uparrow)$ and $1\pi(\downarrow)$ near the center of atom of Fe, C, and O, respectively [Fig. 7(c)]. For $2\pi^*$ PDOS($\downarrow$), the relative intensity at the peak of −1.70 and −0.59 eV is almost the same at the substrate side of the O atom (−1.0, −1.5 Å). Above the O atom position, however, the intensity at the peak of −1.70 eV becomes dominant. This is easy to understand because the electronic states at −1.70 eV originate from the interaction with the $d_{xz}$, $d_{z2}$, $d_{yz}$ orbital of the Fe atom, while states at −0.59 eV mainly come from the $d_{xy}$ orbital. At the vacuum side, significant negative spin polarization can be found at both −1.70 and −0.59 eV energy windows. Moreover, the magnitude of spin polarization increases with increasing the height. When the coverage increases to 0.5 ML, the occurrence of split and broadening of peaks is similar to that of LDOS, due to the tilting of CO molecules and CO-CO interaction.

The spin polarization of electrons can be well characterized by a spin-density map. Figures 7(a)–7(d) show the spin densities along a (001) plane at the whole energy region below $E_F$, $4\sigma$, $5\sigma/1\pi$, and $2\pi^*$ energy windows with the CO coverage of 0.25 and 0.5 ML, respectively. The blue (red color) stands for the positive (negative) value of spin density, which suggests the spin-up (spin-down) electron is dominant.

At $4\sigma$ and $5\sigma/1\pi$ states, negative spin density can be observed obviously around O and C sites, while positive spin density appears near the surface Fe atom as shown in Figs. 7(b) and 7(c). This indicates that the more spin-up electrons transfer from the CO molecule to the Fe atom during the bonding process. The spin density of the $4\sigma$ state extends a little more toward the vacuum side due to the $4\sigma$ state originating mainly from the $s$ and $p_z$ orbital of C and O atoms. Above the O atom a small positive density is observed. This

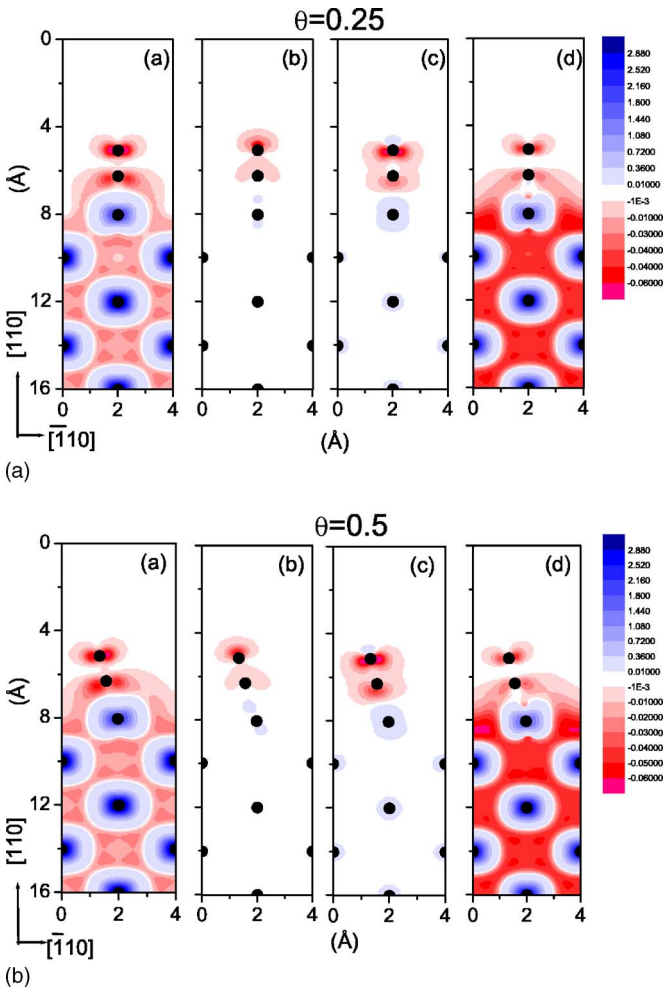


FIG. 7. (Color online) (a) The spin density of CO/Fe(110) with the whole energy range, [(b)–(d)] for $4\sigma$, $5\sigma/1\pi$, and $2\pi^*$ energy window. The top and bottom panels stand for CO coverage of 0.25 and 0.5 ML, respectively.

may come from the $5\sigma$ state but not the $1\pi$ state [see Fig. 7(c)], because the $p_z$ orbital belonging to the $5\sigma$ state extends along the $z$ direction, while $p_x$ and $p_y$ orbitals contributing to the $1\pi$ state are parallel to the surface. Since the $2\pi^*$ state aligns energetically closely with the $d$ band of the Fe substrate, the main characteristic of the substrate is kept as that at whole energy region below $E_F$, including positive spin polarization around the Fe sites and negative spin density at the interstitial region. The clean negative spin polarization at the outside of the substrate results from the backdonation of spin-down electrons.

Now, we turn to compare our calculated results with the SPMDS observations. As mentioned above, as exposure of CO increases, the dominant deexcitation process becomes the AD mechanism. The SPMDS spectra in this process reflect the main features of the density of occupied states of adsorbed molecules (if the ejection probability is approximately the same for surface electronic states at around the interaction surface for $He^*$). The PDOS in the vacuum region shows peaks at an energy region of −10.0–−8.5 eV, −7.0–−5.0 eV, and −2.0–$E_F$. This is consistent with the SPMDS peaks at 4.0, 7.0, and 12.5 eV, since the kinetic energy of 14.5 eV corresponds to the $E_F$. Our calculated results of spin density indicate clearly that even at the low coverage of 0.25 ML, negative-spin polarization extends towards the vacuum side for all three states. This is consistent with the positive asymmetry of the SPMDS, since the $1s$ hole of the $He(2^3S)$ atom, which is filled by a surface electron, has an opposite spin to the incited $He^*$ atom.[47] Besides this, a significant difference between PDOS(↓) and PDOS(↑) at the $2\pi^*$ state gives a reasonable explanation of the large SPMDS asymmetry at the $2\pi^*$ level.

## VI. CONCLUSION

The spin-polarized electronic structure of CO molecules on the Fe(110) surface has been investigated by SPMDS measurements and first-principles calculations. The $2\pi^*$ peak is clearly observed at SPMDS spectra. Negative-spin polarization has been detected for the surface electrons at the energies of −10.0–−8.5 eV, −7.0–−5.0 eV, and especially −2.0 to $E_F$. Theoretical calculations of the spin-density and PDOS in the vacuum region well support those negative-spin polarizations. The electron donation and backdonation between adsorbed CO molecules and Fe substrate are displayed visibly with the subtracted density maps.

## ACKNOWLEDGMENTS

This work was partly supported by a JSPS grant of Japan, the Deutsche Forschungsgemeinschaft through SFB 216, the Nuclear Research Program of the MEXT, and the Atomic Energy Commission of Japan and National Natural Science Foundation of China (Grant No. 60306006).

*Author to whom correspondence should be addressed. Email address: YAMAUCHI.Yasushi@nims.go.jp

[1] B. Gumhalter, K. Wandelt, and P. Avouris, Phys. Rev. B **37**, 8048 (1988).
[2] D. W. Moon, S. L. Bernasek, D. J. Dwyer, and J. L. Gland, J. Am. Chem. Soc. **107**, 4363 (1985).
[3] D. W. Moon, S. L. Bernasek, J. P. Lu, J. L. Gland, and D. J. Dwyer, Surf. Sci. **184**, 90 (1987).
[4] J. P. Lu, M. R. Albert, and S. L. Bernasek, J. Phys. Chem. **94**, 6028 (1990).
[5] S. D. Cameron and D. J. Dwyer, Langmuir **4**, 282 (1988).
[6] M. Getzlaff, D. Egert, P. Rappolt, M. Wilhelm, H. Steidl, G. Baum, and W. Raith, J. Magn. Magn. Mater. **140-144**, 727 (1995).
[7] S. Förster, G. Baum, M. Müller, and H. Steidl, Phys. Rev. B **66**, 134427 (2002).
[8] M. S. Hammond, F. B. Dunning, G. K. Walters, and G. A. Prinz, Phys. Rev. B **45**, 3674 (1992).

[9] T. Suzuki, M. Kurahashi, and Y. Yamauchi, Surf. Sci. **476**, 63 (2001).
[10] T. Suzuki, M. Kurahashi, X. Ju, and Y. Yamauchi, Surf. Sci. **549**, 97 (2004).
[11] M. Onellion, M. W. Hart, F. B. Dunning, and G. K. Walters, Phys. Rev. Lett. **52**, 380 (1984).
[12] D. E. Jiang and E. A. Carter, Surf. Sci. **570**, 167 (2004).
[13] D. C. Sorescu, D. L. Thompson, M. M. Hurley, and C. F. Chabalowski, Phys. Rev. B **66**, 035416 (2002).
[14] A. Stibor, G. Kresse, A. Eichler, and J. Hafner, Surf. Sci. **507-510**, 99 (2002).
[15] M. Getzlaff, D. Egert, H. Steidl, G. Baum, and W. Raith, Z. Phys. D: At., Mol. Clusters **30**, 245 (1994).
[16] H. Steidl and G. Baum, *Selected Topics on Electron Physics*, edited by D. M. Campbell and H. Kleinpoppen (Plenum Press, New York and London, 1996), p. 233.
[17] S. W. Wang and G. Ertl, Surf. Sci. **93**, L75 (1980).
[18] D. R. Penn and P. Apell, Phys. Rev. B **41**, 3303 (1990).
[19] G. Wedler and R. Ruhmann, Appl. Surf. Sci. **14**, 137 (1982).
[20] R. V. Culver, J. Pritchard, and F. C. Tompkins, Z. Elektrochem. Ber. Bunsenges. Physik. Chem. **63**, 741 (1959).
[21] K. Y. Yu, W. E. Spicer, J. Lindau, P. Pianetta, and S. T. Lin, Surf. Sci. **57**, 157 (1976).
[22] G. Wedler, K. G. Colb, G. McElhiney, and W. Heinrich, Appl. Surf. Sci. **2**, 30 (1978).
[23] T. U. Nahm and R. Gomer, Surf. Sci. **384**, 283 (1997).
[24] M. Getzlaff, J. Bansmann, and G. Schönhense, J. Magn. Magn. Mater. **140-144**, 729 (1995).
[25] F. Bozso, J. T. Yates Jr., J. Arias, H. Metiu, and R. M. Martin, J. Chem. Phys. **78**, 4256 (1983).
[26] F. B. Dunning and P. Nordlander, Nucl. Instrum. Methods Phys. Res. B **100**, 245 (1995).
[27] W. Sesselmann, B. Woratschek, G. Ertl, J. Küppers, and H. Haberland, Surf. Sci. **146**, 17 (1984).
[28] J. Roussel, C. Boiziau, R. Novolone, and C. Reynaud, Surf. Sci. **110**, L636 (1981).
[29] H. Conrad, G. Ertl, J. Küppers, W. Sesselmann, and H. Haberland, Surf. Sci. **121**, 161 (1982).
[30] G. Kresse and J. Furthmüller, Phys. Rev. B **54**, 11169 (1996).
[31] G. Kresse and J. Furthmüller, Comput. Mater. Sci. **6**, 15 (1996).
[32] J. P. Perdew, K. Burke, and M. Ernzerhof, Phys. Rev. Lett. **77**, 3865 (1996).
[33] G. Kresse and D. Joubert, Phys. Rev. B **59**, 1758 (1999).
[34] P. E. Blöchl, Phys. Rev. B **50**, 17953 (1994).
[35] H. J. Monkhorst and J. D. Pack, Phys. Rev. B **13**, 5188 (1976).
[36] C. Kittel, *Introduction to Solid State Physics* (Wiley, New York, 1996).
[37] D. Jiang and E. A. Carter, Surf. Sci. **547**, 85 (2003).
[38] G. Herzberg, *Molecular Spectra and Molecular Structure. I. Spectra of Diatomic Molecules* ( 1950), p. 521.
[39] W. Erley, J. Vac. Sci. Technol. **18**, 472 (1981).
[40] P. J. Feibelman, B. Hammer, J. K. Norskov, F. Wagner, M. Scheffler, R. Stumpf, R. Watwe, and J. Dumesic, J. Phys. Chem. B **105**, 4018 (2001).
[41] W. Riedl and D. Menzel, Surf. Sci. **163**, 39 (1985).
[42] H. Kato, M. Kawai, and J. Yoshinobu, Phys. Rev. Lett. **82**, 1899 (1999).
[43] S. K. Nayak, M. Nooijen, S. L. Bernasek, and P. Blaha, J. Phys. Chem. B **105**, 164 (2001).
[44] D. Spisák and J. Hafner, Phys. Rev. B **64**, 094418 (2001).
[45] Q. Ge, S. J. Jenkins, and D. A. King, Chem. Phys. Lett. **327**, 125 (2000).
[46] G. Blyholder, J. Phys. Chem. **68**, 2772 (1964).
[47] M. Kurahashi, T. Suzuki, X. Ju, and Y. Yamauchi, Surf. Sci. **548**, 269 (2004).